Process Optimization with Acid Functionalised Activated Carbon derived from Corncob for Production of *4-Hydroxymethyl-2,2-Dimethyl-1,3-Dioxolane* and *5-Hydroxy-2,2-Dimethyl-1,3-Dioxane*

Jaspreet Kaur
Dr. B. R. Ambedkar National Institute of Technology Jalandhar
Dr Anil Sarma (anil.sarma16@gov.in)
Sardar Swaran Singh National Institute of Bio-Energy
Prof Mithilesh K Jha
Dr. B. R. Ambedkar National Institute of Technology Jalandhar
Dr Poonam Gera
Dr. B. R. Ambedkar National Institute of Technology Jalandhar

Research Article

Keywords:

Posted Date: January 7th, 2021

DOI: https://doi.org/10.21203/rs.3.rs-139195/v1

Version of Record: A version of this preprint was published at Scientific Reports on April 21st, 2021. See the published version at https://doi.org/10.1038/s41598-021-87622-z.

Abstract

This study focuses on the application of the corncob derived base (NaOH) activated and acid (H2SO4) functionalized carbons for the glycerol valorization to produce 2,2-Dimethyl-1,3-dioxolane-4-methanol (solketal), an oxygenated additive to fuel. The two derived catalysts viz., AAC-CC and AC-CC were subjected to various techniques for the determination of their structural properties and their comparison is made on the basis of characteristics and conversion into the final product. The conjugated boat structure of AAC-CC resulted very high surface area (779.8 m2/g) and higher pore volume (0.428cc/g) of AAC-CC that unveil its suitability as better among the two catalytic pathways during the solketal production. The acidic catalyst shows the highest catalytic activity as compared to basic due to the availability of the more active sites to the catalyst that will help in the reaction for higher conversion. The face cantered composite design (FCCD) of RSM was applied for the optimization of the reaction parameters for the ketalisation reaction. From the optimized results, the acidic catalyst AAC-CC gives higher glycerol conversion, i.e. 80.3% than the basic catalyst AC-CC i.e. 72.12% under the actual laboratory experiment. Moreover, the catalyst could be reused for three consecutive batch reactions without (< 5%) much reduction of activity and no distinctive structural deformity.

Introduction

The use of biodiesel as a renewable fuel which is an alternative to petrodiesel has been recognized as an important transition in the liquid fuel-based locomotives, economy, and environment[1].The main source of the glycerol production is the transesterification process of lipid (oil/fat) during biodiesel production[2]. One mole of glycerol is formed as a by-product from one mole of triglyceride (a lipid molecule) in addition to the three moles of biodiesel.

The crude glycerol obtained from biodiesel plants comprises of many impurities and other chemicals, for instance, methanol, organic and inorganic salts, water, vegetable colours, mono, and di-glyceride traces and soap[3,4]. The superabundance of glycerol from biodiesel manufacturers will lead to the availability of glycerol at a demean price; therefore, it would create a huge market value for the applications of crude glycerol[5].

Thus, upgradation must be needed in the processes for transforming glycerol into a pure form or to other value-added products.The glycerol obtained from the biodiesel industry can be a game-changer if the same is properly processed for value-added chemicals/derivatives.A lot of commodity chemicals can be derived from a highly functionalized glycerol molecule via different pathways such as etherification, esterification, carboxylation, dehydration, hydrogenolysis etc.[6]. One plausible pathway that the glycerol can be converted to five and six-membered oxygen-containing functionalized cyclic compounds reported by several authors is the production of 2,2-Dimethyl-1,3-dioxolane-4-methanol (solketal) via ketalisation. The chemical reaction for the production of two ketal species is shown in Figure 1[7]. Solketal is a ring-

shaped di-ether that has an additional hydroxyl group[8]. It can be used as an additive in gasoline, diesel, or biodiesel to increase ignitability and reduce particulate emission[8].

There are various commercially developed catalysts reported in the literature having different physicochemical properties responsible for the conversion of glycerol to solketal. These catalysts may be either acidic or alkaline in nature and the reactions may be either homogeneously or heterogeneously catalyzed[9]. Oprescu et al. reported the green solid superacid catalyst SO_4^{2-}/SnO_2 for the ketalisaton of glycerol to produce solketal with a yield of 97.5%[10].Rodrigues et al. reported the activated carbons produced from olive stone functionalized with acid groups for solketal production with 97% conversion of glycerol[11]. The Nb–SBA-15 (Nb metal modified SBA-15 catalyst) gives 95% glycerol conversion as reported by Ammaji et al[12]. $Fe(NO_3)_3.9H_2O$ exhibited the highest catalytic activity, virtually converting all the glycerol to solketal, with 95% selectivity as reported by Silva et al.[13]. The OTS-grafted HY (organosilanemodified HY) catalyst reported to have high catalytic activity (89% conversion) at low temperatures as stated by Rahamanet al.[14]. Shirani et al. reported a heterogeneous resin catalyst, i.e., Purolite® PD206 for glycerol conversion to solketal with a 95% yield[15]. A mesoporous phenolsulfonic acid-formaldehyde polymeric acid catalyst was synthesized that provides glycerol conversion of 97% as reported by Laskar et al[16].BEA zeolite and the hierarchical zeolite of MFI structure exhibited a high catalytic activity in solketal production, i.e. almost 85% of glycerol conversion and 98% selectivity to solketalwere achieved as reported by Kowalska-Kuś et al[17].

Various acidic or basic homogeneously or heterogeneously catalyzed conversion processes amongst the reported literature unveil that basic catalysts are considered less active as they provide the lower conversion as compared to the acidic catalysts.As per the literature, the basic oxide catalysts partially leached during the reaction which hinders the separation of the catalyst from the reaction mixture[18]. Also, base catalysts can't give high conversion at lower temperature and for a shorter reaction time that led to the formation of salts[19]. Thus, the acidic catalysts show highest catalytic activity as compared to the basic one and leads to better conversion.

It has been observed from the various reported literature that very few renewable precursors-based catalysts are developed[20]. Among all the catalysts investigated, acid and base activated carbons derived from agricultural waste, i.e. corncob has not been reported yet for the production of solketal.Keeping in view the introduction of cleaner production technology for solketal production using renewable precursor-based catalysts, a locally available, merely a waste lignocellulosic residue corncob was studied for the production of acid and base activated carbon catalyst and reported in this work. This lignocellulosic material consists of cellulose of 40–44%, of hemicellulose of 31–33%, and lignin of 16–18[21]. Complete physicochemical characterization of the prepared carbon catalyst after acid functionalisation (H_2SO_4) (AAC-CC) has been accomplished, presented and discussed in this article. Process optimization under different sets of reaction conditions using response surface methodology (RSM) for ketalisation reaction usingAAC-CC has also not been reported elsewhere except this article along with optimal production of ***4-***

hydroxymethyl-2,2-dimethyl-1,3-dioxolane **and** ***5-hydroxy-2,2-dimethyl-1,3-dioxane*** usingvirtual laboratory setup.

Experimental Section

Ketalization reaction. Glycerol (Sigma Aldrich - 97% purity), Methanol (Sigma Aldrich – 99.5 % purity), Acetone (Sigma Aldrich – 99.5 % purity) is used as available commercially and procured from the Merck Specialists Limited, Mumbai in the chemical conversion division of Sardar Swaran Singh National Institute of Bio-energy, Kapurthala, India. The reaction was carried out in a batch reactor (Figure 3) consist of three round neck flasks of 250 ml with varying reaction parameters such as the molar ratio (glycerol: acetone: methanol), reaction temperature, reaction time, catalyst loading (wt. % w.r.t. glycerol).

Figure 3: Batch reactor setup

The flask was then kept in a beaker of 1000 ml containing water which acted as a water bath. This beaker was then placed on a magnetic plate with stirrer and temperature controller to control the temperature and uniform mixing of the reaction mixture during the reaction. Two necks of the flask were blocked by a flask glass stopper and in one reflux and condenserwas also attached to the flask with the help of the burette stand, to maintain the uniformity of the reaction mixture as methanol and acetone were volatile in nature which may evaporate. The reaction was preceded at 600 rpm.

The reactionsset was performed as per the process optimization described below.

Process Optimization. The ketalization reaction of the glycerol using AAC-CC was optimized using face centered composite design (FCCD) of RSM, Design-Expert software version 8.0 (STAT-EASE Inc., Minneapolis, USA) in terms of process parameters, the molar ratio (X1); time (X2); temperature (X3); catalyst amount (X4) to provide us with the maximum glycerol conversion (RSY) as a response (Y)[22]. Software provided 30 no. of reactions consisting of 24 non-central and 6 central axial points (α=1). Central (axial) points were defined for the authenticity of the model via pure error variance. After completion of each reaction, the samples were collected in microcentrifuge tubes and then centrifuged using 5430 R centrifuge to remove the traces of catalyst present in the sample. The centrifuged samples were then diluted to 100 times and were analyzed using high performance liquid chromatography (HPLC - Agilent Technologies model 1260 Infinityand glycerol conversion was calculated using equation (Eq. 1), from the graph obtained from HPLC.

$$\text{Glycerol Conversion (\%)} = \left[\frac{\text{Peak area of product}}{\text{Peakareaofreactant+Peakareaofproduct}}\right] \text{x } 100 \quad \text{Eq.1}$$

Catalyst characterization. The structural properties of the AAC-CC was characterized using various techniques such as Fourier Transform Infrared Spectroscopy (FTIR), Thermogravimetric Analysis (TGA), X-ray Diffraction (XRD), Surface area analysis (BET), X-ray Photoelectron Spectroscopy (XPS), Field

Emission Scanning Electron Microscopy (FESEM), Transmission Electron Microscopy (HRTEM), Temperature Programmed Desorption (TPD).

FTIR experiments were conducted to identify the functional groups. These were interpreted using a PE IR SUBTECH SPECTRUM ASCII PEDS 4.00 infrared spectrometer with a resolution of $1cm^{-1}$. The materials were mixed with KBr powder pelletized and the pellets were scanned in the IR range from 4000 cm^{-1} to 400 cm^{-1}.

The carbonization behavior of the AC-CC was determined by a simultaneous TG/DTA i.e. DTA with the proven capabilities of the TG measurement capabilities, providing thermal property information for a variety of samples. This was done using a SII 6300 EXSTAR thermal analyzer. Samples were heated in the temperature range from 35 °C to 900 °C at a constant heating rate of 5 °C/minute in nitrogen with 200 ml/min flow rate.

Nitrogen adsorption-desorption measurement was carried out using a BET surface area analyzer by St 2 on the NOVA touch 2LX instrument. The samples were degassed for 3 hours at 180 °C on the degassed port. The linear part of the BET equation was used to determine the specific surface area.

The wide-angle X-ray diffraction pattern of the AC-CC was observed on Bruker XRD diffractometer using Cu-Kα radiation with a wavelength of 1.54 and F as a filter. The scanning angle (2θ) range was kept between 10° to 80°.

Scanning electron micrographs (SEM) and elemental analysis of the activated carbon were performed using Nova Nano FE-SEM 450 (FEI) coupled with EDX analyzer of ultra-high-resolution characterization in an accelerating voltage of 15.0 kV.

Transmission Electron Microscopy (HRTEM) study was done with a TEM TECNAI G2 20 S-TWIN (FEI) electron microscope. A drop of the powdered sample was dispersed into ethanol and then dropped onto a carbon-coated copper grid. The high resolution of the analyzer was provided with a voltage of 200 kV.

The presence of surface groups with Carbon, Sulphur, Oxygen, Silicon, and Sodium was identified and confirmed by X-ray photoelectron spectroscopy (XPS) using PHI 5000 Versa Probe III model.

The acidity of the catalyst surfaces was studied using Temperature program desorption (TPD) and performed using BEL's new fully-automated catalyst analyzer (BELCAT II) with NH3 as investigating molecule and He as a carrier gas. The desorption of NH_3 was performed after flushing using carrier gas up to temperature 600 °C at a heating rate of 10 °C/min.

Results

Catalyst characterization using different physical and adsorption techniques. The plausible structures of the single-molecule of the derived catalyst (Figure 4) and supramolecular structure (Figure 5) have been drawn using the ChemDraw software using the composition obtained from SEM-EDX analysis.

The surface groups present in the carbon material produced were characterized and identified using different techniques before its utilization for the ketalization reaction. The presence of different functional groups in the structure was identified from an extensive study of FTIR and XPS analysis. The XRD patterns of the catalyst showed the amorphous nature of the carbon material.

The microstructural evaluation was done using Scanning Electron Microscopy (SEM) and the SEM micrographs of the derived functionalised activated carbon has been shown in Figure 6. It can be observed from the picture that AAC-CC has developed a conjugated boat-like structure having a rough or uneven surface with cavities and cracks in the external surface and random pore size distribution[23]. The elemental analysis was performed using energy-dispersive (SEM-EDX) and the elemental composition of the sample showed the presence of Carbon, Oxygen, Sulfur in AAC-CC. Carbon is present in the highest amount i.e. 90.99% in AAC-CC responsible for the higher glycerol conversion[24]. Thus, carbonization is confirmed in the sample[25] (Table 1) with minimum carbon loss in AAC-CC.

Table 1: Elemental analysis of the catalyst

AAC-CC		
C	O	S
90.99	8.40	0.52

The TEM micrograph of the AAC-CC is shown in Figure 7(a) while AC-CC in Figure 7(b). The TEM results are in good agreement with SEM results showing the porosity of the produced catalysts. The images revealed a complete porous carbon structure for both the activated carbons even at higher magnification. The existence of the pore structure of the catalyst is attributed to the NaOH activation adopted during the synthesis of the AC-CC catalyst[26,27] and H_2SO_4 activation AAC-CC as shown in the images[28]. The sizes and uniformity envisage that the glycerol molecule with a size of 0.5-0.6 nm can easily fit and escape from these pores where the active functional groups are present that facilitates the group transferand cyclization reactions of glycerol.

FT-IR spectra shows a broad peak at around 3426.50 cm^{-1} in AAC-CC(Figure 8) for stretching of –OH bond of alcohol.The 2924.72 cm^{-1} peak shows the aliphatic C-H stretching vibration in AAC-CC. The peak at 2856.82 cm^{-1}show the vibration of the -OH group attached to ring carbon in the derived catalyst. There is a broad peak at 1694.28 cm^{-1}which shows the stretching of the C=C due to the influenced functionalities. The sharp band at 1595.93 cm^{-1} corresponds to stretch probably from an amide in the acid- activated catalyst[30].The peaks at 1457.57 cm^{-1}, 1381.38 cm^{-1}, and 1084.04 cm^{-1} show the C-C stretching vibration of the chain hydrocarbon parts due to different structural influences, C-H stretching vibration in alkanes or an alkyl group and C-S group, respectively in base-activated catalyst[29]. The peak at 779.62 cm^{-1} shows the absorption of the SiO_2 and the 548 cm^{-1} peak shows the C-H stretching of aromatic compounds[29,31].The additional bands at 1171.17 cm^{-1} and 1123.8 cm^{-1} shows the stretching of

sulfonated groups in acid activated carbon[20]. The functional groups represent the chemically active components of the catalyst that accelerates the rate of reaction.

The values of specific surface area calculated using the BET equation are presented in Table 2 together with the values of the total pore volume, Vp, taken at P/Po = 0.99, and average pore radius pore size distribution curves for activated carbon samples have been obtained from BJH calculation method[32].

The adsorption-desorption isotherm of AAC-CC is classified as type IV and reveals a hysteresis loop of H4 type implies to narrow slit pores including the pores in the micropore region as shown in Figure 9[33]. H4 loops are often found with the micro-mesoporous carbons.

Table 2: Surface area, pore volume and pore size parameters

Corncob derived catalysts	Specific surface area -A_{BET} (m^2/g)	Pore volume – Vp (cc/g)	Pore radius – r (nm)
Acid Activated Carbon	779.831	0.428	0.001
Base Activated Carbon	13.901	0.011	1.223

A very high surface area and higher pore volume of AAC-CC unveil its suitability as the better of the two catalytic pathways during the solketal production as shown in Table 2.

The thermal behavior of the AAC-CC (TG and DTA) was observed in the temperature range from 30 °C to 900 °C. TG and DTA curves show the weight loss from 30-903 °C for AAC-CC as shown in Figure 10. The weight loss at the initial stage up to 100 °C shows the removal of moisture while volatilization occurs at about 150 °C in AC-CC[29]. In AAC-CC, the weight loss from 200-300 °C corresponds to the decomposition of the sulfonated groups. The weight loss from 300-400 °C is due to the loss of cellulosic materials. The prominent desorption occurs between 400-481°C[34]. The weight loss at 600-700 °C shows the decomposition of the produced carbon and the weight loss at 800-900°C shows the decomposition of the organic components. After 600 °C, the fusion of the carbon occurs till 800 °C and 800-900 °C is the ash fusion temperature.

The acidic sites of the catalysts are determined by NH_3-TPD as these are the active sites responsible for the conversion of glycerol to solketal at a modest temperature[35]. The acidic strength of solid acid catalysts in the NH_3-TPD profiles can be classified into three regions depending on their strength in the temperature range. These acidic sites are denoted as weak (150–300 °C), moderate (300–450 °C), and strong (450–650 °C)[12]. The desorption peak of NH_3-TPDfor AAC-CC shows a weak acidic site at 147.1 °C while showing a sharp peak at 605°C with higher intensity having strong acidic strength (Figure 11). The total acidic amount of 0.187 mmol/g was observed for the acidic site.

The surface chemistry has been studied using XPS and concluded the presence of groups attached in the AAC-CC and confirmation of the groups present are shown in Figure 12(a), (b), (c)&(d).

Discussions

Catalyst Activation and functionalization: The carbon percentage in AC-CC was 78%, whereas in AAC-CC it is 91%. Moreover, the sodium, oxygen and silica content are drastically reduced in the AAC-CC. This is confirmed from the EDX and XPS data that the percentage of C increases by 13 % after acid functionalization of the NaOH activated carbon. Moreover, the Rib shaped AC-CC has been converted to conjugate boat structure in AAC-CC, resulting high porosity and 50-60-fold increased surface area. This may be attributed to the following basic reactions for the removal of silica and Na bonded with AC-CC in step -II production of activated carbon.

$$\text{AC-CC } SiO_2 + H_2SO_4 \longrightarrow SiO_2\text{-}H_2SO_4(gel) \xrightarrow{\text{washing}} \text{Boat shaped AAC-CC}$$

$$\text{AC-CC Na} + H_2SO_4 \longrightarrow NaHSO_4 \xrightarrow{\text{washing}} \text{Boat shaped AAC-CC}$$

Effect of reaction parameters for solketal production. In the present work, Response surface methodology (RSM) was employed to optimize the values of process parameters for the ketalization reaction to get the improved glycerol conversion with derived catalystsby correlating the experimentaland predicted values; numerical optimization method andanalysis of standard error in the obtained values; quadraticregression in the model through desirability function as 0.999 forprecision of the results. In addition, possible interactions betweenprocess factors were also determined for their overall influence on progress of the process.After completion of optimization of the process via RSM, the obtained 30 sets of experiments were conducted in actual laboratory conditions for the production of solketal. The obtained results are summarised in Table 2 in supplementary section (SS-I) in the form of observed values of RSY against the coded values.

The effect of reaction parameters (molar ratio, time, temperature and catalyst amount) on RSY were also studied by plotting three-dimensional (3-D) surface curves shown oin SS-I, Figure 2. Plotting 3-D response surface between two independent variables is the best way to explicate their interaction effects on dependent variable. The conversion of glycerol via ketalisation reaction was observed to be influenced by parameters within the range: molar ratio (1:2:2 to 1:8:8), time (1 to 3 hours), temperature (50 to 150 °C) and catalyst amount (1 to 5 wt.%). The highest value of RSY was found to be 80.3% against the predicted value of 73.807% for solketal production corresponding to the parameters with molar ratio-1:8:8, for 2 hours at 100 °C and 3wt.% catalyst loading. It was observed that further increase in the reaction temperature associated only with lower glycerol conversion and was confirmed in table 2 in SS-I. From the shape of the 3-D surface plots, it was concluded that the effect of molar ratio on glycerol conversion dominates when compared with the effect of other variables like conversion increases with increase in molar ratio but time has not showed the significant change in conversion as shown in figure 2(a), SS-I.

These results have been found in concordance with the optimized results that obtained by RSM employing ANNOVA (Analysis of Variance).

The catalytic activity was also studied for the ketalization reaction i.e. conversion of glycerol to solketal using the derived functionalise catalyst obtained from corn cob. In order to check the stability of the catalyst and effectiveness of the active sites of the catalyst, a reusability study was carried out[29].The catalyst was separated from the reaction mixture after the completion of the reaction by filtering the reaction mixture using filter paper. It was then washed with ethanol 3-4 times and then dried in an oven at a temperature of 90°C. The study showed that the catalyst can be reused up to three consecutive batch reactions without much loss of the activity (<5%) and no distinctive structural deformity.

Conclusions

Conversion of glycerol to solketalusing acid functionalized activated corncob-based carbon as catalyst is greener pathway and possible. The acid-activated carbon has a higher surface area, pore-volume, and strong acidic sites that catalyze the reaction with a higher conversion rate as compared to alkali-activated carbon. Molar ratio of the reactants (glycerol: acetone:methanol) has the significant effect upon the ketalization reaction. The catalyst can be reused and a prototype can be developed in near future for cleaner production of solketal from crude glycerol.

Declarations

Acknowledgement:

The first author thankfully acknowledges the Ph.D. fellowship funded from MHRD, Govt. of India and supported by Dr. B R Ambedkar NIT, Jalandhar. The first author also acknowledges SSS-NIBE, Kapurthala for their infrastructural support, analytical support and guidance for carrying out this work.

References

1. Monteiro, M. R., Kugelmeier, C. L., Pinheiro, R. S., Otávio, M. & César, S. Glycerol from biodiesel production : Technological paths for sustainability. *Renew. Sustain. Energy Rev.***88**, 109–122 (2018).
2. Anitha, M., Kamarudin, S. K. &Kofli, N. T. The potential of glycerol as a value-added commodity. *Chem. Eng. J.***295**, 119–130 (2016).
3. Hájek, M. &Skopal, F. Treatment of glycerol phase formed by biodiesel production. *Bioresour. Technol.***101**, 3242–3245 (2010).
4. Yang, F., Hanna, M. A. & Sun, R. Yang et al. 2012 value added use crude glycerol. *Biotechnol. Biofuels***5**, 1–10 (2012).
5. U.S.C. Bureau, Glycerol Imports and exports, 2015.

6. Brandner, A., Lehnert, K., Bienholz, A., Lucas, M. & Claus, P. Production of biomass-derived chemicals and energy: Chemocatalytic conversions of glycerol. *Top. Catal.***52**, 278–287 (2009).
7. Moreira, M. N., Faria, R. P. V., Ribeiro, A. M. & Rodrigues, A. E. Solketal Production from Glycerol Ketalization with Acetone: Catalyst Selection and Thermodynamic and Kinetic Reaction Study. *Ind. Eng. Chem. Res.***58**, 17746–17759 (2019).
8. Alsawalha, M. Catalytic Activity and Kinetic Modeling of Various Modules HZMS-5 and Treated MCM-41 Catalysts, for the Liquid-Phase Ketalization of Glycerol With Acetone. *Front. Chem.***7**, (2019).
9. Kaur, J., Sarma, A. K., Jha, M. K. & Gera, P. Valorisation of crude glycerol to value-added products: Perspectives of process technology, economics and environmental issues. *Biotechnol. Reports***27**, e00487 (2020).
10. Oprescu, E. E., Stepan, E., Dragomir, R. E., Radu, A. &Rosca, P. Synthesis and testing of glycerol ketals as components for diesel fuel. *Fuel Process. Technol.***110**, 214–217 (2013).
11. Rodrigues, R., Gonçalves, M., Mandelli, D., Pescarmona, P. P. & Carvalho, W. A. Solvent-free conversion of glycerol to solketal catalysed by activated carbons functionalised with acid groups. *Catal. Sci. Technol.***4**, 2293–2301 (2014).
12. Ammaji, S., Rao, G. S. & Chary, K. V. R. Acetalization of glycerol with acetone over various metal - modified SBA - 15 catalysts. *Appl. Petrochemical Res.***8**, 107–118 (2018).
13. da Silva, M. J., Rodrigues, A. A. & Pinheiro, P. F. Solketal synthesis from glycerol and acetone in the presence of metal salts: A Lewis or Brønsted acid catalyzed reaction? *Fuel***276**, 118164 (2020).
14. Rahaman, M. S. *et al.* Hydrophobic functionalization of HY zeolites for efficient conversion of glycerol to solketal. *Appl. Catal. A Gen.***592**, 117369 (2020).
15. Shirani, M., Ghaziaskar, H. S. & Xu, C. Optimization of glycerol ketalization to produce solketal as biodiesel additive in a continuous reactor with subcritical acetone using Purolite® PD206 as catalyst. *Fuel Process. Technol.***124**, 206–211 (2014).
16. Laskar, I. B., Rajkumari, K., Gupta, R. &Rokhum, L. Acid-Functionalized Mesoporous Polymer-Catalyzed Acetalization of Glycerol to Solketal, a Potential Fuel Additive under Solvent-Free Conditions. *Energy and Fuels***32**, 12567–12576 (2018).
17. Kowalska-Kuś, J., Held, A. &Nowińska, K. A continuous-flow process for the acetalization of crude glycerol with acetone on zeolite catalysts. *Chem. Eng. J.***401**, (2020).
18. Sivaiah, M. V., Robles-Manuel, S., Valange, S. &Barrault, J. Recent developments in acid and base-catalyzed etherification of glycerol to polyglycerols. *Catal. Today***198**, 305–313 (2012).
19. Tao, M., Zhang, D., Guan, H., Huang, G. & Wang, X. Designation of highly efficient catalysts for one pot conversion of glycerol to lactic acid. *Sci. Rep.***6**, 1–13 (2016).
20. Mäki-arvela, P., Kumar, N., Mikkola, J. & Deka, D. Biodiesel production from acid oils using sulfonated carbon catalyst derived from oil-cake waste. *"Journal Mol. Catal. A, Chem.* (2013). doi:10.1016/j.molcata.2013.09.031

21. Wang, L. *et al.* An environmentally friendly and efficient method for xylitol bioconversion with high-temperature-steaming corncob hydrolysate by adapted Candida tropicalis. *Process Biochem.***46**, 1619–1626 (2011).
22. Hans, M. *et al.* Liquid ammonia pretreatment optimization for improved release of fermentable sugars from sugarcane bagasse. *J. Clean. Prod.* 123922 (2020). doi:10.1016/j.jclepro.2020.123922
23. Yakout, S. M. & Sharaf El-Deen, G. Characterization of activated carbon prepared by phosphoric acid activation of olive stones. *Arab. J. Chem.***9**, S1155–S1162 (2016).
24. Feng, P., Li, J., Wang, H. & Xu, Z. Biomass-based activated carbon and activators: Preparation of activated carbon from corncob by chemical activation with biomass pyrolysis liquids. *ACS Omega***5**, 24064–24072 (2020).
25. Solomon, O. *et al.* Sustainable conversion of agro-wastes into useful adsorbents. *Appl. Water Sci.* (2016). doi:10.1007/s13201-016-0494-0
26. Momodu, D. *et al.* Activated carbon derived from tree bark biomass with promising material properties for supercapacitors. *J. Solid State Electrochem.***21**, 859–872 (2017).
27. 27.Kumar, P. *et al.* Characterization, activity and process optimization with a biomass-based thermal power plant's fly ash as a potential catalyst for biodiesel production. *RSC Adv.***5**, 9946–9954 (2015).
28. Jyoti, L., Boro, J. & Deka, D. Review on latest developments in biodiesel production using carbon-based catalysts. *Renew. Sustain. Energy Rev.***29**, 546–564 (2014).
29. Kaur, J. Rib shaped carbon catalyst derived from Zea.*RSC Adv.*43334–43342 (2020). doi:10.1039/d0ra08203a
30. Ekpete, O. A., Marcus, A. C. &Osi, V. Preparation and Characterization of Activated Carbon Obtained from Plantain (Musa paradisiaca) Fruit Stem. *J. Chem.***2017**, (2017).
31. Tsai, W. T., Chang, C. Y., Wang, S. Y. & Chang, C. F. Cleaner production of carbon adsorbents by utilizing agricultural waste corn cob. **32**, 43–53 (2001).
32. Bedia, J., Peñas-Garzón, M., Gómez-Avilés, A., Rodriguez, J. &Belver, C. A Review on the Synthesis and Characterization of Biomass-Derived Carbons for Adsorption of Emerging Contaminants from Water. *C***4**, 63 (2018).
33. Thommes, M. *et al.* Physisorption of gases, with special reference to the evaluation of surface area and pore size distribution (IUPAC Technical Report). *Pure Appl. Chem.***87**, 1051–1069 (2015).
34. Nda-Umar, U. I., Ramli, I., Muhamad, E. N., Taufiq-Yap, Y. H. &Azri, N. Synthesis and characterization of sulfonated carbon catalysts derived from biomass waste and its evaluation in glycerol acetylation. *Biomass Convers. Biorefinery* (2020). doi:10.1007/s13399-020-00784-0
35. Zbair, M. *et al.* Structured carbon foam derived from waste biomass: application to endocrine disruptor adsorption. *Environ. Sci. Pollut. Res.***26**, 32589–32599 (2019).
36. Kumar, A. & Prashant, S. Preparation and Characterization of Musa balbisianaColla Underground Stem Nano-material for Biodiesel Production Under Elevated Conditions. (2014). doi:10.1007/s10562-014-1206-8

Figures

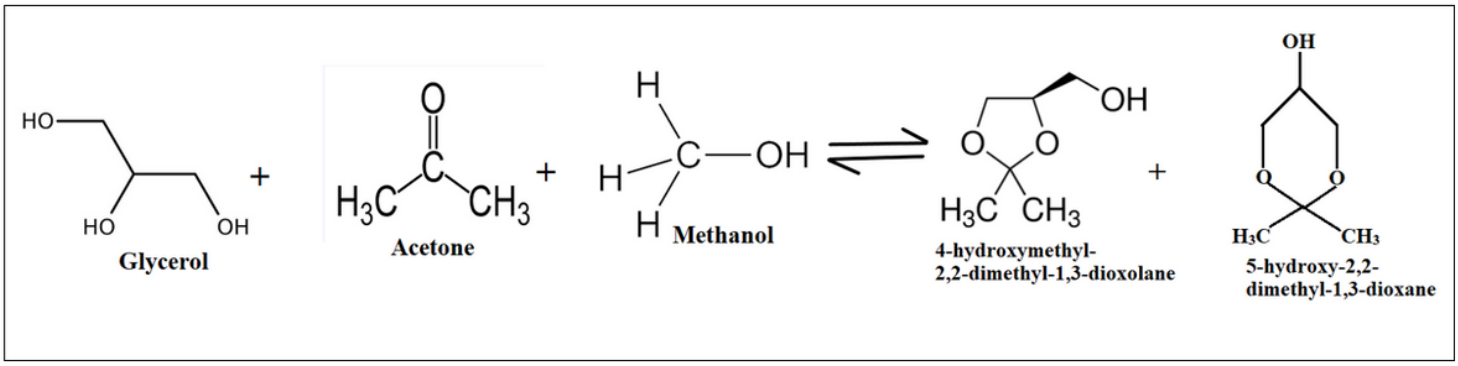

Figure 1

Ketalization reaction for the production of ketals from glycerol

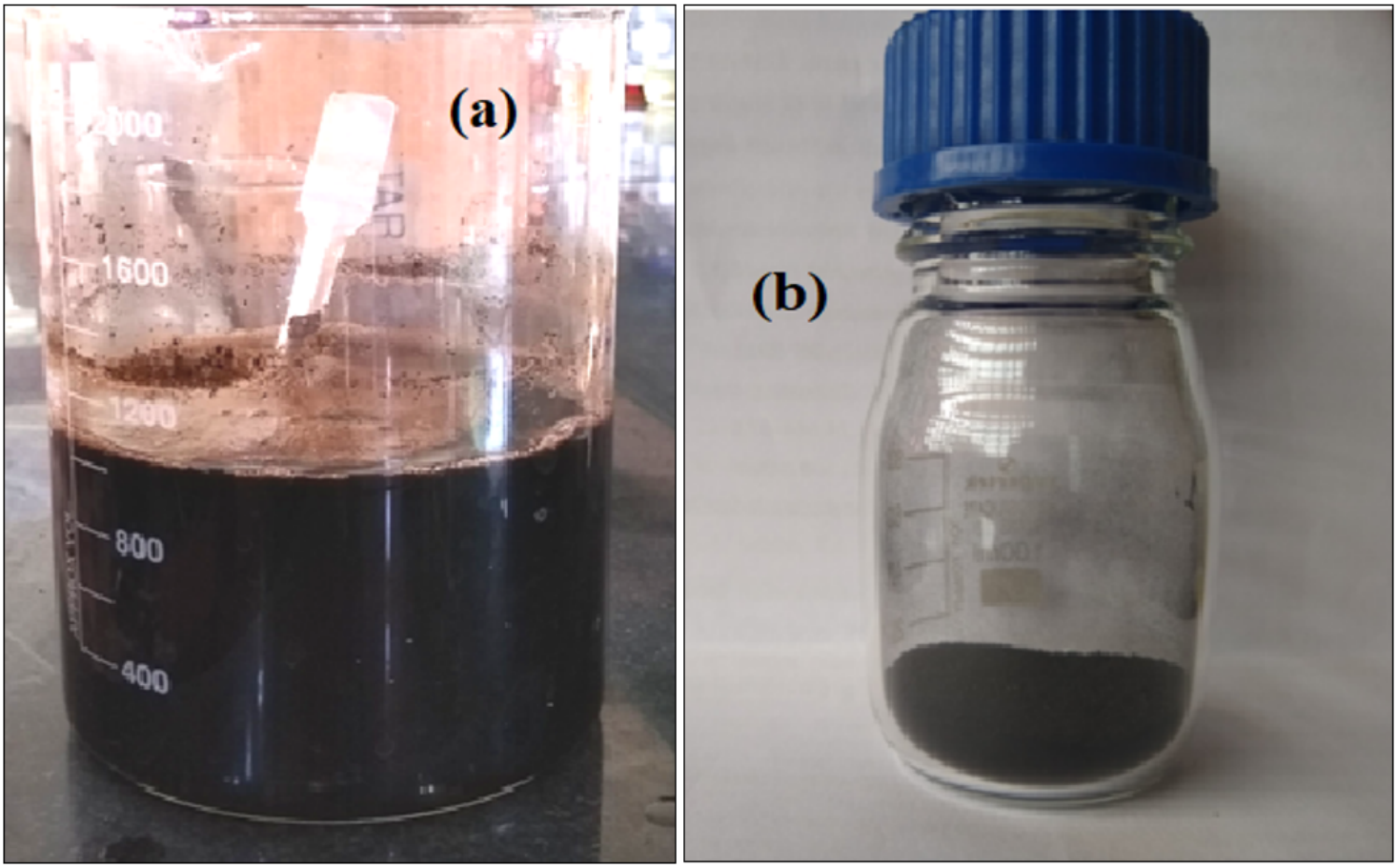

Figure 2

(a) Carbonised carbon after filtration dipped in the Sulphuric acid (b) Final acid functionalized activated carbon stored in the air tight bottle

Figure 3

Batch reactor setup

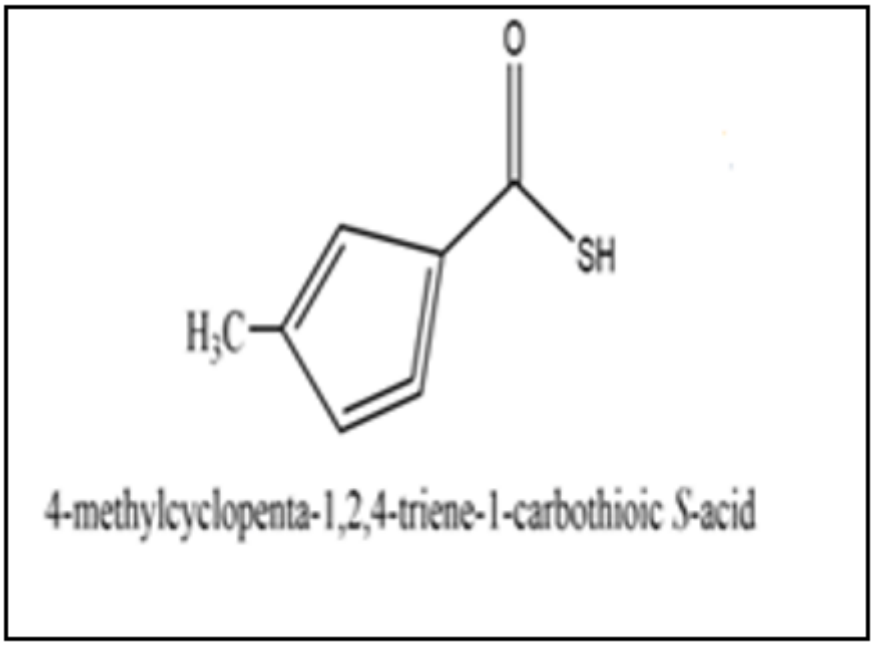

Figure 4

Plausible structure of a single molecule ofAcid Functionalised Activated Corncob

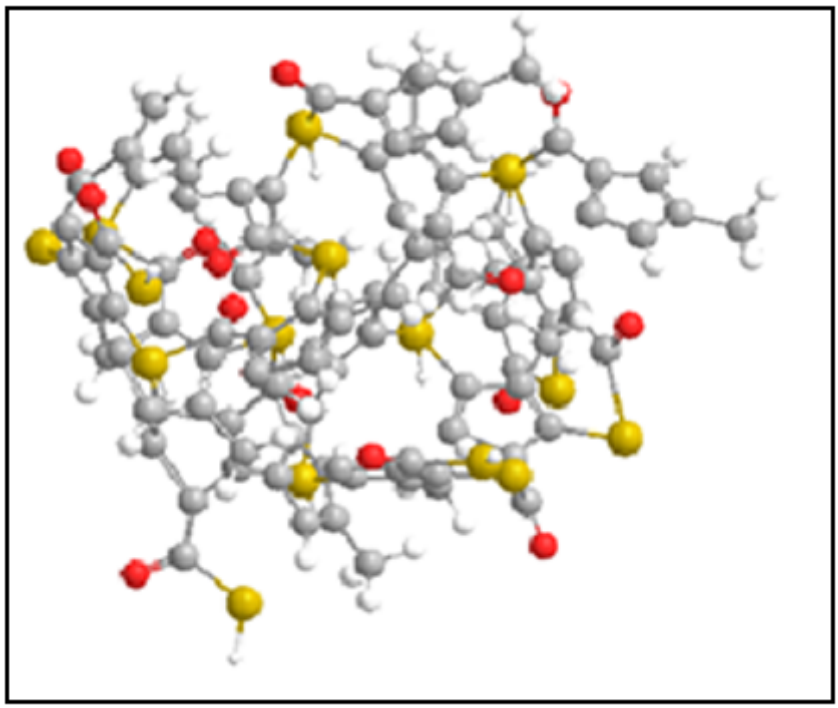

Figure 5

3-D view of agglomerated structure of Acid Functionalised Activated Corncob

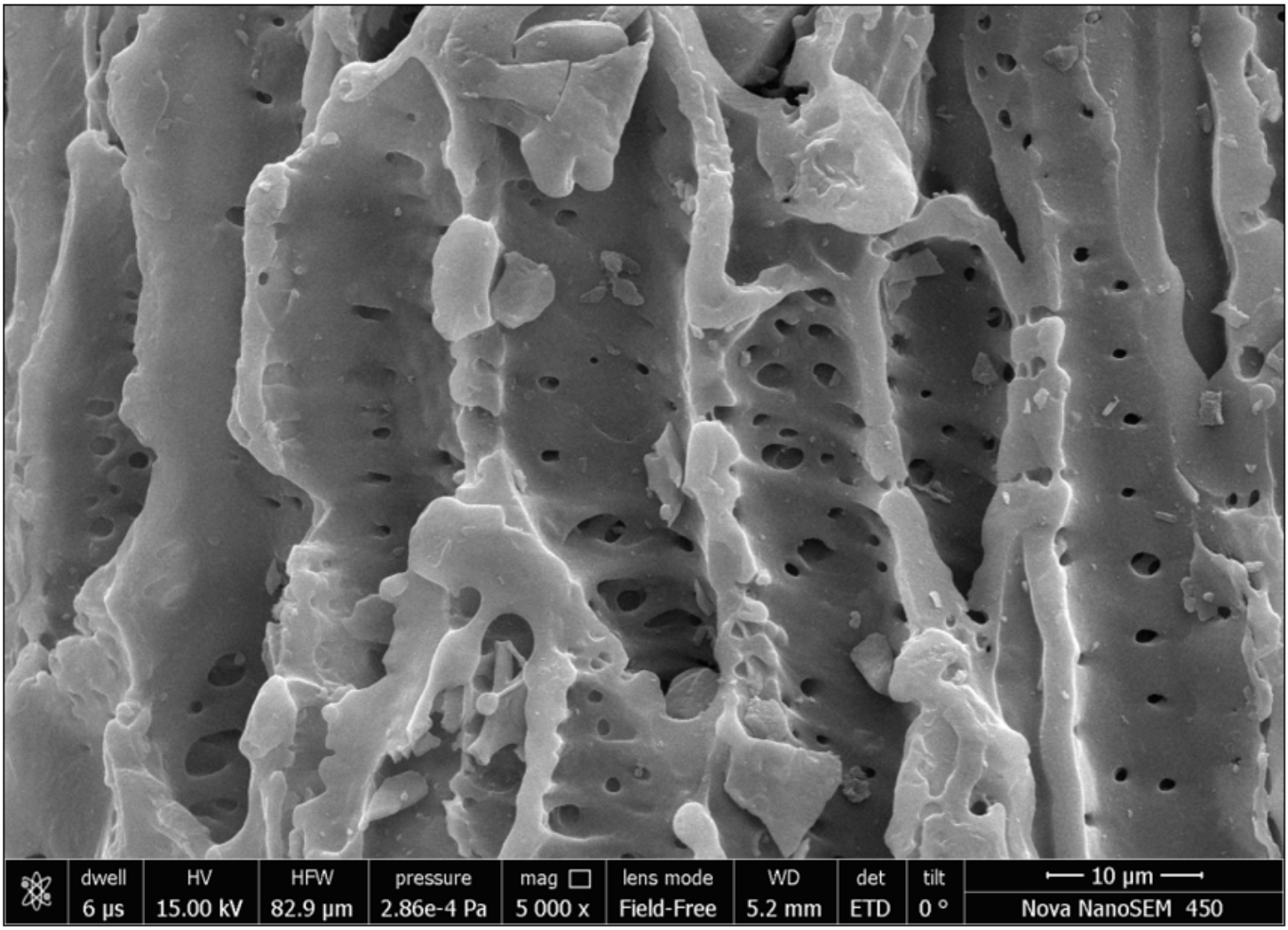

Figure 6

SEM images of derived catalysts Acid FunctionalizedActivated Corncob

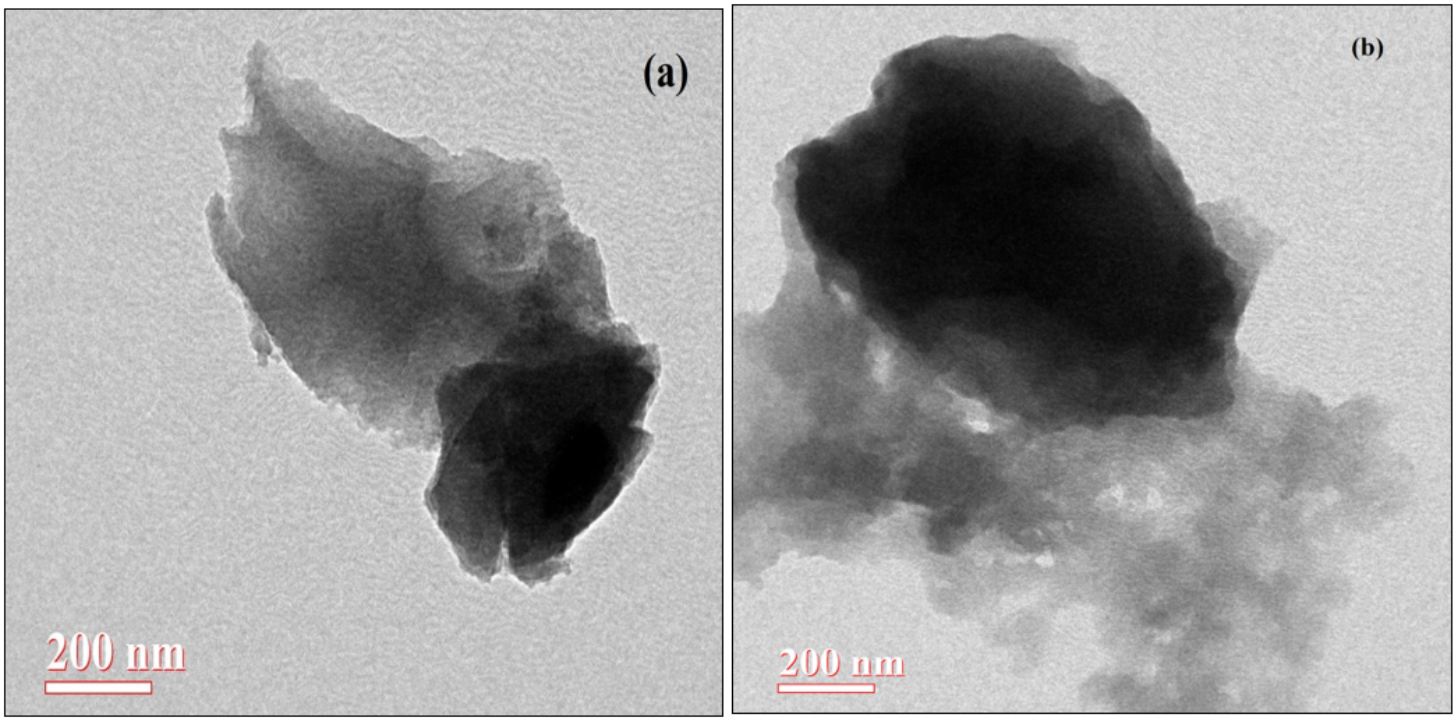

Figure 7

TEM images of the catalysts (a) AAC-CC (b) AC-CC29

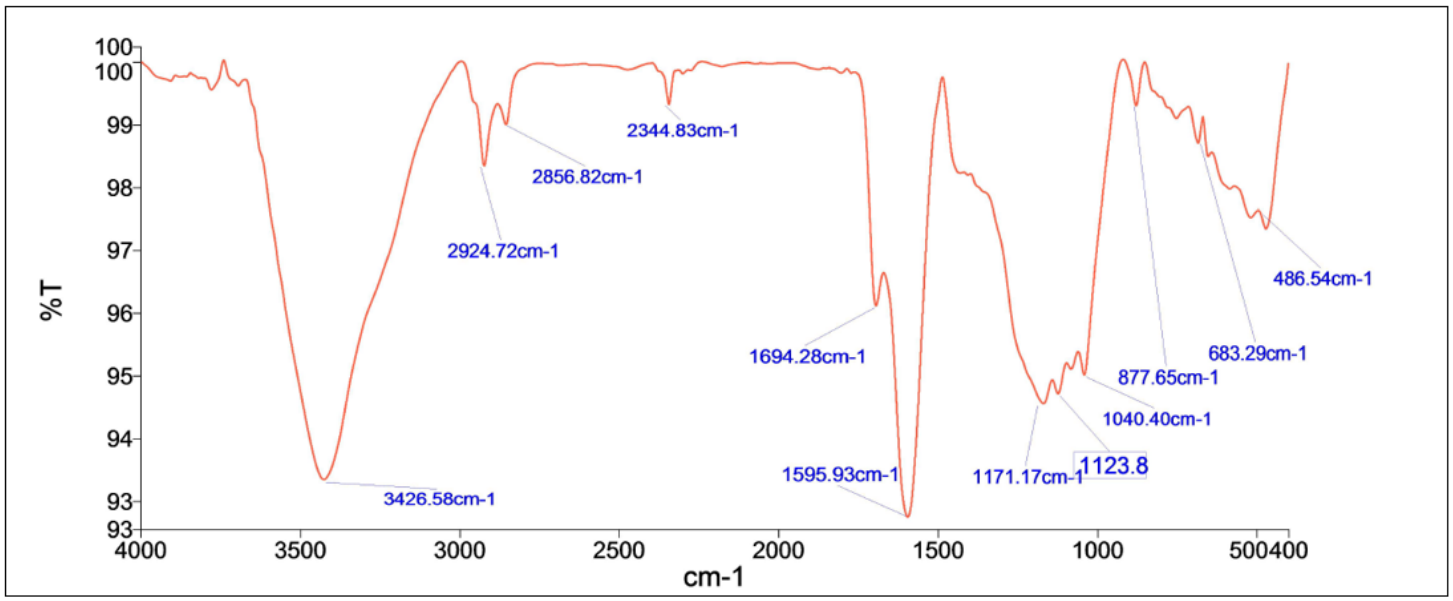

Figure 8

FTIR patterns of the derived activated carbons AAC-CC

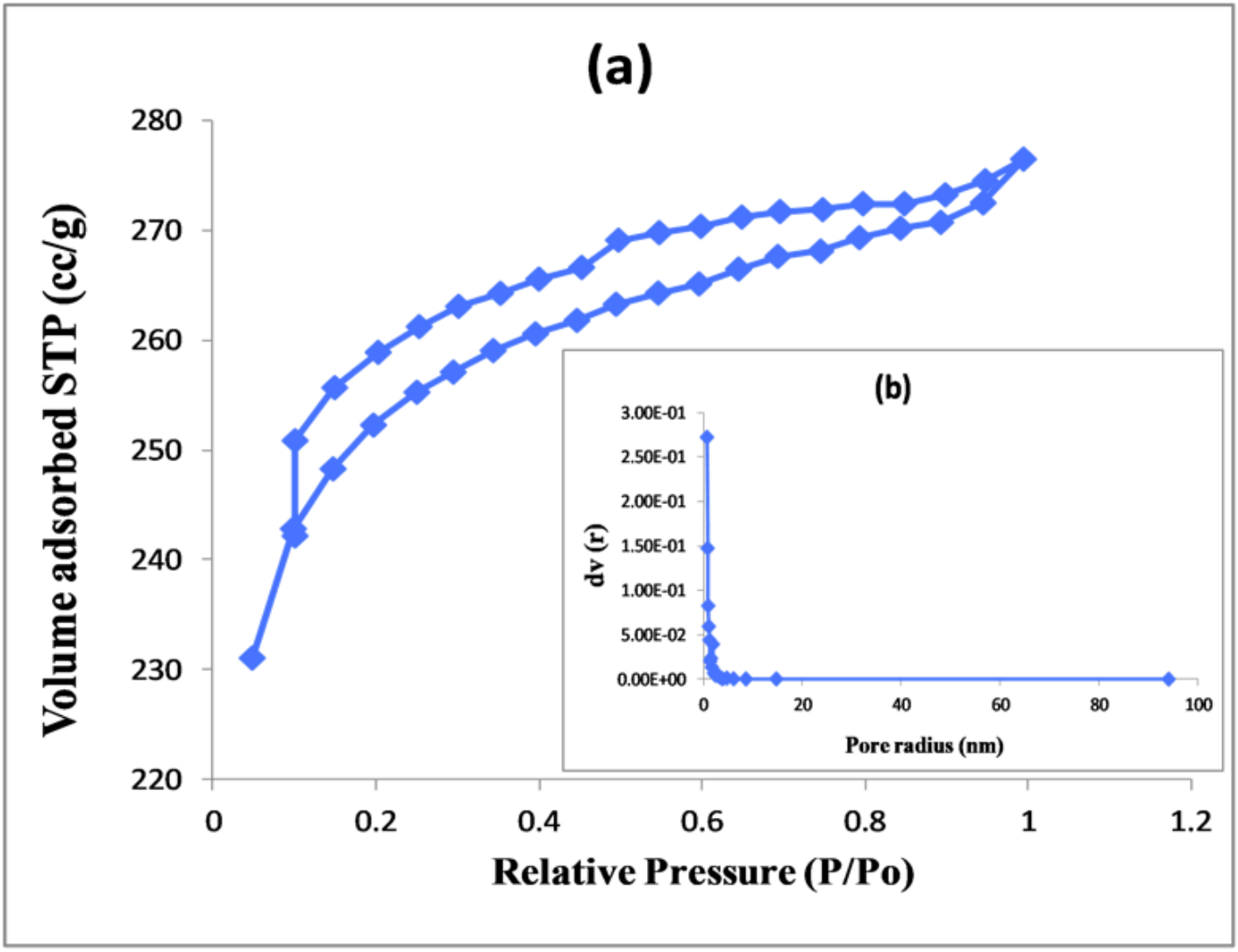

Figure 9

For acid activated carbon (a) N2 adsorption-desorption isotherm (b) Pore size distribution

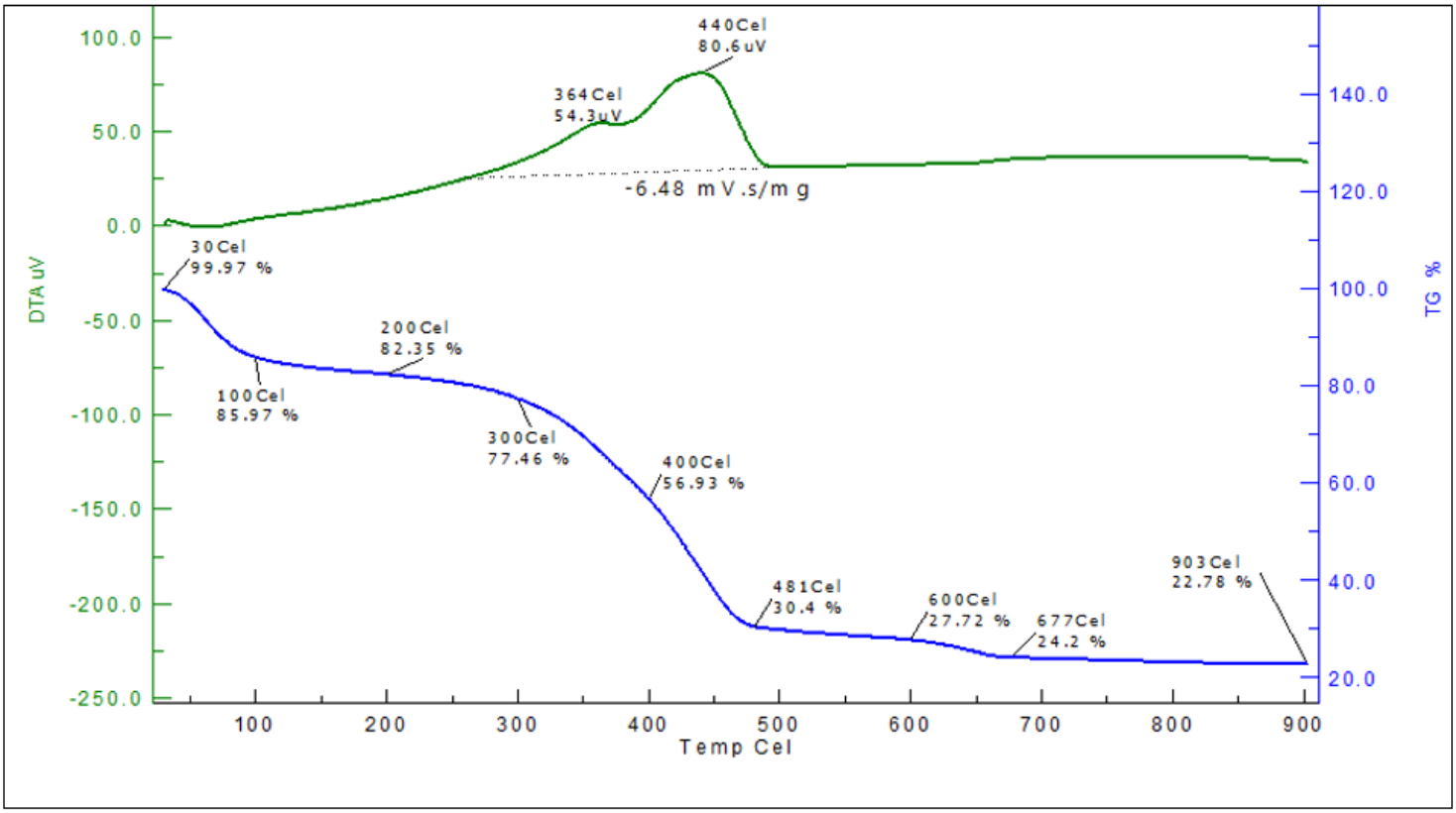

Figure 10

TG-DTA curve of theAAC-CC catalysts

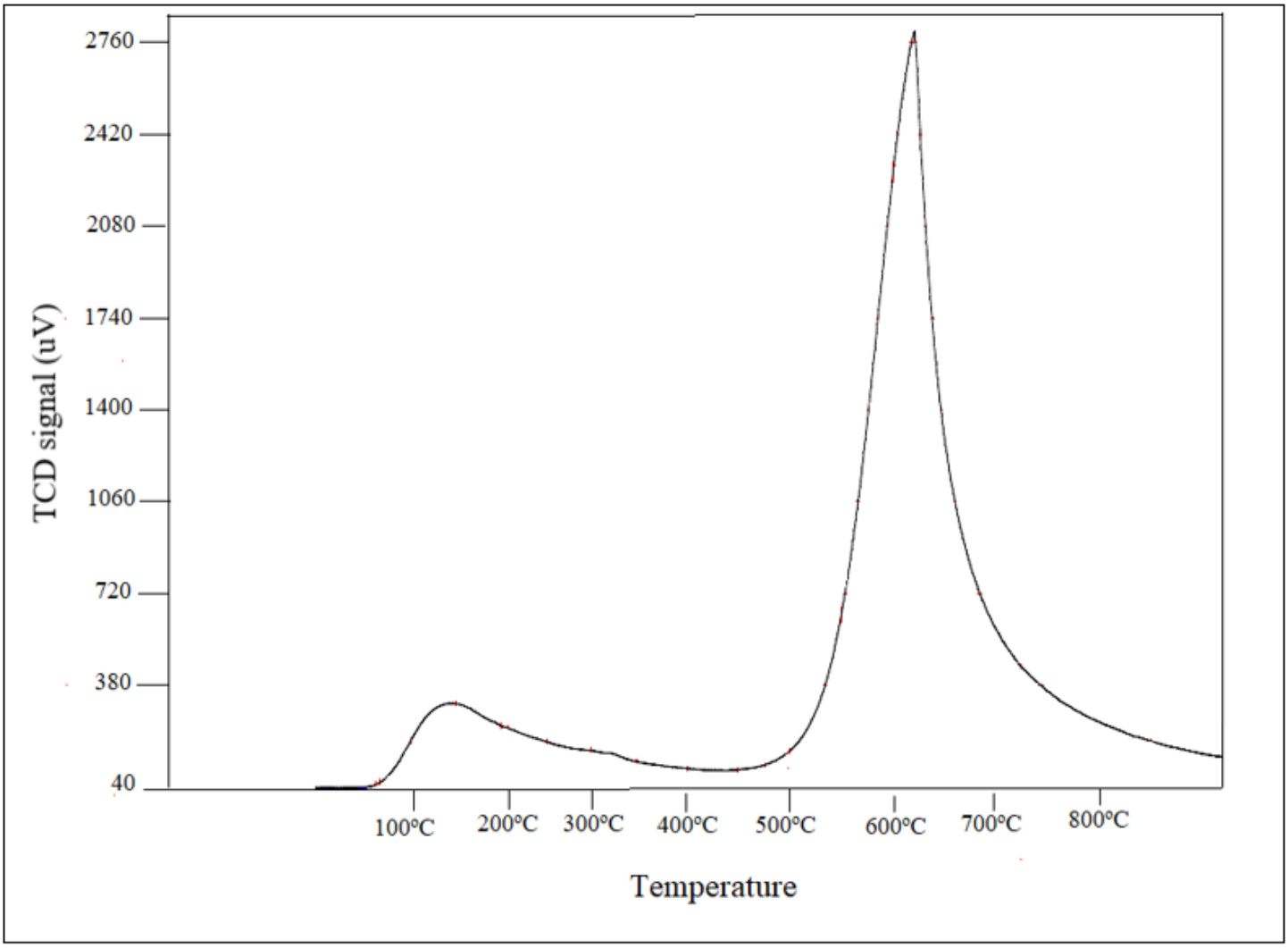

Figure 11

TPD-NH3 of acid activated carbon AAC-CC

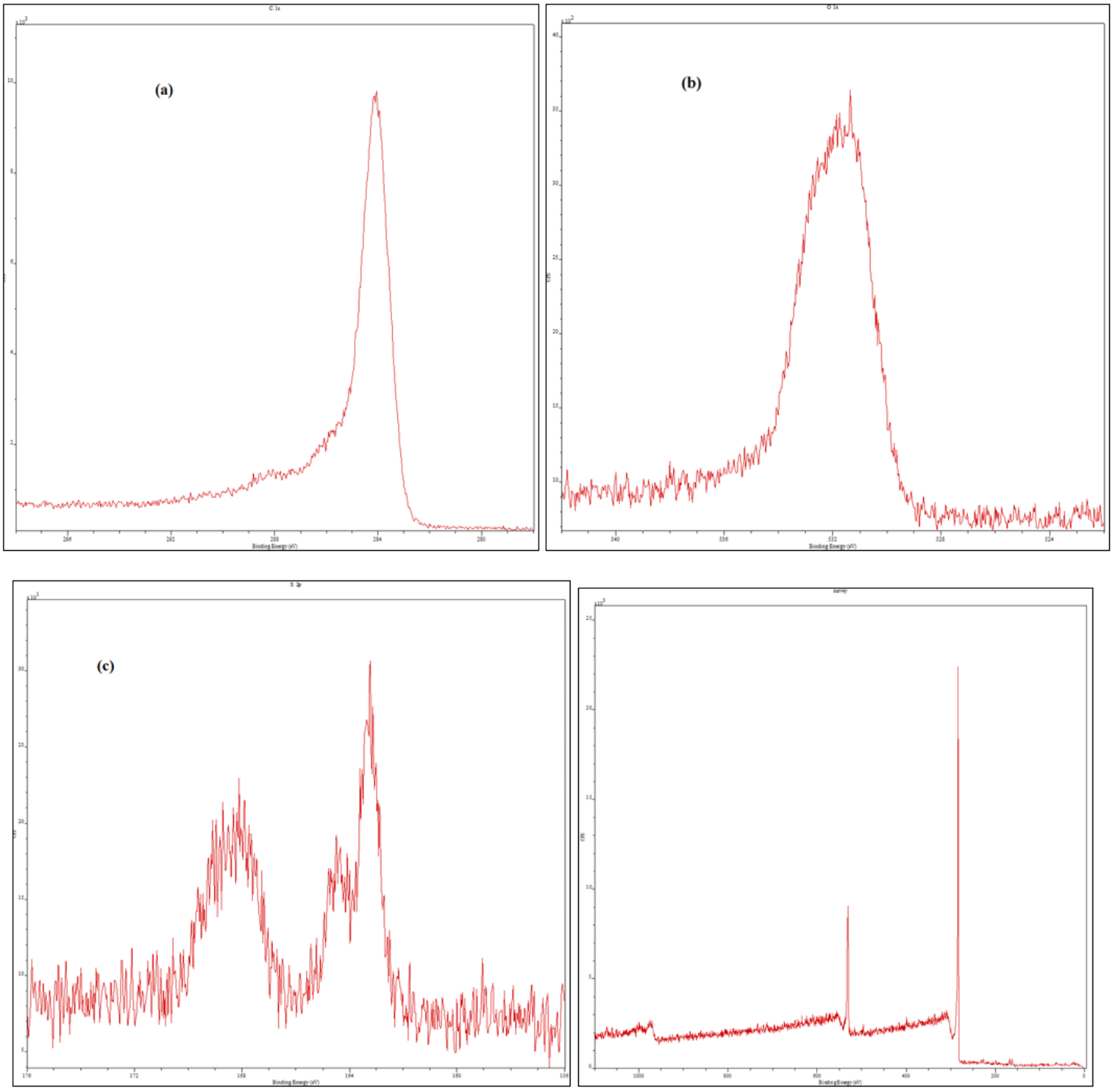

Figure 12

Deconvolution of (a) Carbon, (b) Oxygen, (c) Sulphur and (d) XPS spectrum

Supplementary Files

This is a list of supplementary files associated with this preprint. Click to download.

- SupplementaryInformation.docx